Journal Pre-proof

An enzyme linked aptamer photoelectrochemical biosensor for Tau-381 protein using AuNPs/$MoSe_2$ as sensing material

Xu Hun (Conceptualization) (Methodology) (Writing - review and editing) (Formal analysis) (Data curation) (Writing - original draft) (Visualization) (Investigation), Xiaohui Kong (Supervision) (Validation) (Writing - review and editing) (Project administration) (Funding acquisition)

PII: S0731-7085(20)31552-1

DOI: https://doi.org/10.1016/j.jpba.2020.113666

Reference: PBA 113666

To appear in: *Journal of Pharmaceutical and Biomedical Analysis*

Received Date: 20 July 2020

Revised Date: 26 September 2020

Accepted Date: 28 September 2020

Please cite this article as: Hun X, Kong X, An enzyme linked aptamer photoelectrochemical biosensor for Tau-381 protein using AuNPs/$MoSe_2$ as sensing material, *Journal of Pharmaceutical and Biomedical Analysis* (2020), doi: https://doi.org/10.1016/j.jpba.2020.113666

An enzyme linked aptamer photoelectrochemical biosensor for Tau-381 protein using AuNPs/$MoSe_2$ as sensing material

Xu Hun[1], Xiaohui Kong

Key Laboratory of Optic-electric Sensing and Analytical Chemistry for Life Science, MOE; Shandong Key Laboratory of Biochemical Analysis; Key Laboratory of Analytical Chemistry for Life Science in Universities of Shandong; State Key Laboratory Base of Eco-chemical Engineering; College of Chemistry and Molecular Engineering, Qingdao University of Science and Technology, Qingdao 266042, China

[1]Corresponding author, E-mail: hunxuprof@outlook.com

Highlights

- **AuNPs/$MoSe_2$ NSs modified electrode**
- **A PEC platform for Tau-381 protein using AuNPs/$MoSe_2$ NSs as photoactive substance**
- **A low noise was obtained.**
- **LOD 0.3 fM for Tau-381 protein.**

Abstract

Alzheimer's disease is a worldwide health problem and it has attracted extensive attention. Tau protein is an important biomarker in the pathogenesis of Alzheimer's disease. Herein, we devise a in situ enzyme catalysis generating electron donor photoelectrochemical (PEC) biosensor for Tau-381 protein. Tau-381 protein aptamer is immobilized onto the surface of AuNPs/$MoSe_2$ nanosheets modified electrode. In the presence of Tau-381 protein, an aptamer-protein duplex is formed. Meanwhile, the Tau-381 antibody and the protein G/AP (protein G labeled with alkaline phosphatase) are captured with the affinity interaction between Tau-381 protein and Tau-381 antibody, Tau-381 antibody and protein G/AP. The electron donor, ascorbic acid, is in situ produced by the catalyzing of ascorbic acid 2-phosphate in the PEC detection solution. As a result, low blank noise and strong photocurrent response are engendered. The photocurrent response is related to the concentration of Tau-381 protein. The detection range of Tau-381 protein is from 0.5 fM to 1.0 nM with detection limit of 0.3 fM. This in situ generating electron donor PEC biosensor can detect various targets by simply alternating antibody, antigen, or aptamer commercially. Thus, this work represents a simple and general sensing protocol.

Key words: Aptamer, Photoelectrochemistry, Tau-381, Selenide molybdenum, In-situ, Ascorbic acid

Introduction

The world's aging population is huge, and the number of Alzheimer's disease (AD) patients increases every year, so AD needs our more attention [1]. AD is unremitting and neurodegenerative disorder which was also called senile dementia, it causes cognitive and memory impairment by destroying brain cells [2]. Except for the testing of neurofibrillary tangles and plaques in brain tissue, there is no other effective diagnosis method for AD. In view of the high costs and poor cure for AD, safe and effective detection for AD need to be developed. The study discovered that the total amount of Tau protein in their cerebral spinal fluid and plasma of AD patients had an increase compared with the controls of the same age group [3]. That's because Tau protein plays a very important role in the structure of the microtubules, such as it can maintain the integrity of microtubule [4]. In the brains of AD patients, more than 20 Tau protein residues are phosphorylated. In comparison, 8-10 of these residues are phosphorylated in healthy individuals. Tau protein loses the ability to combine with microtubules because it is phosphorylated. And phosphorylated Tau protein in nerve cells could mutuality combine with each other to form "knots" named as neurofibrillary tangles. These neurofibrillary tangles stop the transportation of essential supplies in the cells and eventually cause cell death. Thus, Tau protein is an important biomarker for AD. Six isoforms of Tau protein contain 352, 381, 383, 410, 412, 441 amino acids, respectively. And the Tau-381 protein is one of the six known variants, and its amino acids length ranges from 352 to 441. Commercially available ELISA kits cannot distinguish the different variants, because the common epitope sites for antibody pairs across all species.

It is important to develop sensitive strategy for disease prevention and treatment [5, 6]. The methods currently used for disease detection are electrochemical [7], chemiluminescence [8], fluorescence [9], and photoelectrochemical (PEC) [10]. Tau protein plays a crucial role in the pathogenesis of AD. Some analytical techniques were used to dete[6]ct Tau protein, such as surface-enhanced Raman scattering (SERS) [11], surface plasmon resonance (SPR) [12], enzyme-linked immunoabsorbent assay (ELISA) [13], single molecule ELISA digital array technology [14], bioreceptor array chip platform [15]. However, no PEC method is used to detect Tau-381 protein at present.

Aptamers are single-stranded DNA/RNA molecules (20-80 nucleotides) isolated or evolved from random oligonucleotide pools by exponential enrichment in vitro selection technique (SELEX) that can specifically bind to target molecules [16]. These oligonucleotides through self-folding can form tertiary or secondary structures, which can not only distinguish the fine structure and spatial structure but also match the target molecules. Due to the exhibit affinity and high specificity to the targets, they were used as affinity reagents to achieve the specific recognition and adsorption. All in all, aptamers can apply to biosensors in the diagnosis and treatment of diseases.

$MoSe_2$ was transition-metal dichalcogenides material with semiconductor characteristics [17]. $MoSe_2$ especially possesses higher intrinsic electronic conductivity [18]. $MoSe_2$ is formed by combining Mo atom and Se atom via the strong covalent bonds (Se-Mo-Se) and the layers are bound by weak van der Waals interactions [19].

And this type of weak interaction makes bulk $MoSe_2$ could be exfoliated into $MoSe_2$ nanosheets ($MoSe_2$NSs). More importantly, $MoSe_2$ has a narrow direct optical band gap at 1.7–1.9 eV [20]. $MoSe_2$ might be an appropriate material for the fabrication of PEC biosensor.

In this study, we developed a method with enzyme linked aptamer PEC biosensor (ELA-PEC biosensor) for Tau protein detection. This ELA-PEC biosensor uses commercial aptamer, antibody and protein G labeled with alkaline phosphatase (protein G/AP) coupled with AuNPs/ $MoSe_2$NSs modified electrode for the detection of Tau-381 protein. Thus, a sensitive ELA-PEC biosensor was achieved; besides, an ELA-PEC biosensor achieves the detection of various targets by alternating the antibody, the antigen, or the aptamer.

2 Experimental

2.1 Reagents and materials

Selenide Molybdenum ($MoSe_2$), Chloroauric acid ($HAuCl_4 \cdot 4H_2O$), Ascorbic acid (AA), Ascorbate alkaline phosphate (AAP) and N, N‑Dimethylformamide (DMF) were obtained from J&K Chemical Ltd. (Shanghai, China). Sodium citrate and Magnesium nitrate ($Mg(NO_3)_2$) were obtained from Shanghai Reagent Company (Shanghai, China). Tris(hydroxymethyl) aminomethane (Tris) is obtained from Aladdin Chemicals Co. Ltd. (Shanghai, China). Sodium dihydrogen phosphate ($NaH_2PO_4 \cdot 2H_2O$), Disodium hydrogen phosphate ($Na_2HPO_4 \cdot 12H_2O$), Potassium ferrocyanide [$K_4Fe(CN)_6$] and Potassium ferricyanide [$K_3Fe(CN)_6$] were obtained from Sinopharm Chemical Reagent Co. Ltd., (Shanghai, China). Human Serum Albumin (HSA), Tau-410, Tau-441, alpha-1 antitrypsin (AAT), Tau-381 protein and Tau-381 antibody were obtained from Abcam (Cambridge, UK). Recombinant protein G labeled with alkaline phosphatase (protein G/AP) was obtained from Shanghai Zibo Biotechnology Co., Ltd. (Shanghai, China). 6-Mercapto-1-hexanol (MCH) and DNA aptamer were obtained from Sangon Biotech Co., Ltd. (Shanghai, China), and the aptamer sequence is 5′-SH-GCGGAGCGTGGCAGG-3′ [12]. All chemical reagents are analytical grade. Various aqueous solutions were prepared by ultrapure water (18 MΩ).

2.2 Apparatus

All the PEC measurements and electrochemical impedance spectra (EIS) experiment were carried out on a CHI 660E electrochemical workstation (CHI Instrument, Shanghai, China). A standard three-electrode system with a 10 W LED lamp was used to PEC measurement. A carbon paste electrode (CPE) or modified CPE was used as the working electrode; a saturated calomel was used as the reference electrode and a platinum wire was used as the auxiliary electrode. A KQ-500B sonifier was used for the ultrasonic process. The surface morphology characterization of bulk $MoSe_2$, $MoSe_2$NSs and AuNPs/$MoSe_2$NSs was observed by JSM-6700F scanning electron microscopy (SEM, JEOL, Japan). The surface morphology characterization of bulk $MoSe_2$, $MoSe_2$NSs and AuNPs/$MoSe_2$NSs was conducted on a JEM-3010 transmission electron microscope (TEM, JEOL, Japan).

2.3 Preparation of modified electrodes

$MoSe_2$NSs was obtained via a simple ultrasonic exfoliation method from bulk $MoSe_2$ with DMF solvent. $MoSe_2$NSs was obtained after ultrasonic exfoliation for 10 h, and it

was centrifuged for 20 min at 14,000 rpm to remove the DMF. Finally, the precipitated $MoSe_2$NSs was obtained. Afterwards, the $MoSe_2$NSs was rinsed three times with ethanol. Then AuNPs/$MoSe_2$NSs was synthesized by the sodium citrate reduction method [21, 22]. The details were as follows: $MoSe_2$NSs and chloroauric acid of different mass ratio of 1:3.75, 1:2.5, 1:1.875 were mixed separately (volume, 1:1) and the mixture solution was boiled with continued vigorous stirring. Under vigorous stirring, the sodium citrate (6.6 mg of sodium citrate corresponds to 10 mg of chloroauric acid) was added to the boiled mixture solution. After a 30 min reaction, the AuNPs/$MoSe_2$NSs was obtained and it was washed three times with DMF. Eventually, the AuNPs/$MoSe_2$NSs was diluted with DMF and stored at 4 °C. 15 μL AuNPs/$MoSe_2$NSs solution (2.5 mg mL^{-1}) was dropped on a CPE surface and dried at room temperature and the AuNPs/$MoSe_2$NSs/CPE was obtained.

2.4 Fabrication of the PEC biosensor

The DNA aptamer was prepared with a 10 mM Tris-HCl buffer (pH 7.4). And 15 μL aptamer (1.0×10^{-6} mol L^{-1}) was coated at the AuNPs/$MoSe_2$NSs/CPE. Then the modified AuNPs/$MoSe_2$NSs/CPE was incubated for 24 h at room temperature to modify the aptamer via Au-S bond. After incubation, the unbonded aptamer was rinsed three times using 10 mM Tris-HCl buffer (pH 7.4). Subsequently, the modified electrode was immersed into 1 mM MCH solution and washed by phosphate buffer (10 mM, pH 7.4). The aptamer/AuNPs/$MoSe_2$NSs/CPE was obtained. Then aptamer/ AuNPs/$MoSe_2$NSs/CPE was first incubated with sample (35 μL) which contained different concentrations of Tau-381 protein at 37 °C for 30 min and then rinsed with 0.1 M phosphate buffer (pH 7.4) three times. Thereafter, the modified electrode was incubated with 25 μg mL^{-1} Tau antibody (35 μL) for another incubation at 37 ºC for 1 h, and then rinsed with 0.1 M PBS (pH 7.4) three times to remove the unbound and physically absorbed antibody. Subsequently, the modified electrode was incubated with 8 μg mL^{-1} protein G/AP (35 μL) for another incubation at 37 ºC for 1 h, and then rinsed with 0.1 M PBS (pH 7.4) three times. Finally, the assembled electrodes were inserted into 0.1 M Tris-HCl solution (10 mM Tris-HCl, pH 9.8 contained 0.1 mM $Mg(NO_3)_2$ contained 0.1 M AAP) at 37 ºC for 1 h. Then the PEC responses of the electrodes were measured.

2.5 PEC measurement

The different concentrations of Tau-381 protein were monitored by the photocurrent response in Tris-HCl solution contained AAP at the potential of 0.2 V. The light was switched off-on-off for 10 s - 10 s - 10 s under bias potential.

2.6 Detection of Tau-381 protein in real sample

The human serum was obtained from Qingdao Center Medical Hospital (Qingdao, China. Ethical Committee License Number: QDCH 2018-05). We evaluate the practical utility of ELA-PEC biosensor by the detection of Tau-381 protein in real samples via standard addition method. Auxiliary detection was evaluated by comparing the concentration of Tau-381 protein in the serum of healthy people and AD's patients. The different concentrations of Tau-381 protein (0.5 pM, 5.0 pM, 10.0 pM, were added to the healthy human serum diluted 100-fold with 0.1 M phosphate buffer. And the serum from AD's patient was also diluted 100-fold with 0.1 M PBS.

3 Results and discussion

3.1 Characterization of $MoSe_2$NSs and AuNPs/$MoSe_2$NSs

In this enzyme linked aptamer PEC biosensor commercial $MoSe_2$ was used as the photoactive material. The morphology of the $MoSe_2$ was characterized by SEM and TEM. As shown in **Figure 1 (A, B, D, E)**, the bulk $MoSe_2$ was thick and it became thinner after ultrasonic exfoliation. The exfoliated thin-layer $MoSe_2$, $MoSe_2$NSs, have a larger specific surface area than bulk $MoSe_2$. And the $MoSe_2$NSs have an increased photocurrent response because it can accelerate the transportation of electrons. The morphology of the AuNPs/$MoSe_2$NSs was characterized by SEM and TEM. As shown in **Figure 1 (C, F)**, it showed that AuNPs were well dispersed on $MoSe_2$NSs. It showed AuNPs were uniform spheres and with an average diameter of 15 ± 3 nm (**Figure S9**). The exciting AuNPs are conducive to bind aptamer and increase electrical conductivity. In addition, **Figure 1 (G)** shows the Elemental mapping spectrum of Mo, Se and Au. As shown in **Figure 1 (H)**, the energy-dispersive spectrometry (EDS) demonstrated the existence of Mo, Se and Au elements from the sharp peaks. It can be seen from the SEM, TEM, EDS and Elemental mapping that the AuNPs/$MoSe_2$NSs is synthesized successfully.

Figure 1 Here

3.2 Principle of enzyme linked aptamer PEC biosensor strategy

As shown in the schematic diagram, aptamer was first immobilized onto the surface of electrode (**Scheme 1**). In the presence of Tau-381 protein, the conformation is changed by combining with target protein and it forms an aptamer-protein duplex. Concurrently the Tau-381 antibody and the protein G/AP were captured with the affinity interaction between Tau-381 protein with Tau-381 antibody, Tau-381 antibody with protein G/AP. Due to the high-efficient catalysis of enzyme, a large number of substrates, AAP, are in situ catalyzed into electron donor, AA. In this way, PEC signal was produced. Because of the absence of electron donor in the PEC detection cell, there is no PEC signal in the absence of Tau-381 protein. Low blank noise is gained and is good for improving detection sensitivity. With the commercial reagents, aptamer, Tau-381 antibody and protein G/AP, an enzyme linked aptamer PEC biosensor for Tau-381 protein was established. The resulting Tau-381 protein concentration was photoelectrochemically detected using a PEC reader.

Scheme 1. Here

3.3 The properties of enzyme linked aptamer PEC biosensor

AuNPs/$MoSe_2$NSs show better PEC response than bulk $MoSe_2$ **(Figure 2 (A))**. In order to immobilize the aptamer, AuNPs were chemically deposited onto $MoSe_2$NSs. Then AuNPs/$MoSe_2$NSs/CPE was prepared. The PEC properties of the modified electrodes were inspected. It was found that $MoSe_2$NSs/CPE and AuNPs/$MoSe_2$NSs/CPE gave almost a similar PEC response. And their PEC responses are bigger than that of bare CPE **(Figure 2 (A))**. It shows that $MoSe_2$NSs is better to be

applied to PEC biosensor. Then, the mass ratio of $MoSe_2$ to chloroauric acid was studied. It was found that the mass ratio of $MoSe_2$NSs and chloroauric acid of 1:2.5 shows a good PEC response **(Figure 2 (B)).**

Figure 2. Here

To corroborate the feasibility of ELA-PEC biosensor as shown in **Scheme 1**, the target-induced PEC responses were first tested by using a PEC detection biosensor which can collect the PEC response in the presence of Tau-381 protein. As shown in **Figure 3**, an obvious PEC response was recorded (**curve f**). Nevertheless, the PEC response of 0.1 fM target of Tau-381 protein was similar to the PEC noise **(curve g)**. And in the traditional PEC analysis biosensor, the photoactive material was modified onto the electrode, and the enhancer, electron donors or electron acceptors was excited in the detection solution. The high PEC noise was produced although there was no target. High noise is the major factor in reducing sensitivity [23]. The low PEC noise in this enzyme linked aptamer PEC biosensor is good for the improvement of sensitivity.

Next, the ELA-PEC biosensor was studied systematically. Experimentally, the photocurrent responses were recorded while the electrodes were irradiated with LED lamp. As shown in **Figure 3 (A)**, it can be clearly seen that the ELA-PEC biosensor is successful fabricated step by step. The photocurrent of bare CPE was 32.1 nA (**curve a**). After the AuNPs/$MoSe_2$NSs was coated on the surface of CPE, the photocurrent was increased to 189.7 nA (**curve b**). Then aptamer, MCH and Tau-381 protein, antibody was captured on the AuNPs/$MoSe_2$NSs/CPE step by step, the photocurrent was 183.2 nA (**curve c**), 192.7 nA (**curve d**), 190.0 nA (**curve e**). After the protein G/AP being added the PEC signal was 201.3 nA (**curve j**) if there is no AAP. But in the presence of AAP the protein G/AP/antibody Tau-381 protein/MCH/aptamer/AuNPs/$MoSe_2$NSs/CPE produced a high PEC signal (2042.6 nA, **curve f**). While, there is no target the PEC response is 187.2 nA (**curve g**). As is shown above, the concentration of the target being 0.3 fM which is LOD (seen it in the section 3.5), the PEC is 264.3 nA (**curve h**). As for 0.1 fM target which the concentration is reduced to below to LOD, and there is only low PEC signal which is alike to that produced from the AuNPs/$MoSe_2$NSs/CPE (185.8 nA, **curve i**). It suggested that our assumption is realizable. The ELA-PEC biosensor can give a low noise.

Electrochemical Impedance Spectroscopy (EIS) was also used to characterize the stepwise fabrication of the ELA-PEC biosensor. In the EIS, the size of the semicircle diameter can express the strength of the electron transfer resistance (Ret). The EIS plot was illustrated in **Figure 3 (B)**. The interface properties of the electrodes were studied based on the EIS plot. Bare CPE presented a small Ret value (curve a) of 156.3 Ω. After the bare CPE was modified with AuNPs/$MoSe_2$NSs, the modified CPE showed a decreasing Ret value (curve b) of 83.8 Ω, because AuNPs can increase the electrical conductivity. When the MCH, aptamer, Tau-381 protein, Tau antibody and protein G/AP were step by step immobilized onto the AuNPs/$MoSe_2$NSs/CPE, the Ret value gradually increased to around 526.7 Ω (curve c), 660.3 Ω (curve d), 852.2 Ω (curve e),

1327.9 Ω (curve f) and 1694.6 Ω (curve g). The low electron-transfer capacity and the increased steric hindrance of CPE lead to the increased Ret. And the significant change in Ret also can indicate the successful construction of the ELA-PEC biosensor.

Figure 3 Here

3.4 Optimization of experimental conditions

The following parameters were optimized. (a) potential; (b) AuNPs/$MoSe_2$NSs volumes; (c) aptamer concentration; (d) Tau antibody concentration; (e) protein G/AP concentration; (f) catalysis temperature; (g) catalysis time. The respective data and figures are shown in the Supporting Information (**S1, Figure S1~S7**). We found the following experimental conditions gave the best results: (a) potential of 0.2 V; (b) AuNPs/$MoSe_2$NSs volumes of 15 μL; (c) aptamer concentration of 1 μM; (d) Tau antibody concentration of 25 $\mu g \cdot ml^{-1}$; (e) protein G/AP concentration of 8 $\mu g \cdot ml^{-1}$; (f) catalysis temperature of 37 °C; (g) catalysis time of 60 min.

3.5 Application of the enzyme linked aptamer PEC biosensor

To evaluate the analytical performance of the fabricated ELA-PEC biosensor, different concentrations of Tau-381 protein were measured under optimal experimental conditions. With the increased concentrations of Tau-381 protein (0, 0.5 fM, 1.0 fM, 5.0 fM, 10.0 fM, 50.0 fM, 500.0 fM, 5.0 pM, 50.0 pM, 500.0 pM, 1.0 nM) the photocurrent response was increased. Different concentrations of Tau-381 protein were detected in the optimized conditions. As shown in **Figure 4**. The photocurrent response corresponding increased with increasing Tau-381 protein concentration from 0 to 1 nM. The photocurrent responses and the logarithmic value of Tau-381 protein concentrations have a fine linear relationship and the linear regression equation was I/nA=429.0323 log(C)+6924.5699 (C, the concentration of Tau-381 protein, R^2 = 0.9977). The detection limit was calculated as 0.3 fM (3 S/N). Finally, this method being compared with other detection methods for Tau-381 protein was illustrated in **Table 1**. Compared with other methods for Tau protein detection, this ELA-PEC biosensor has a low detection limit. Therefore, this ELA-PEC biosensor is a feasible way to detect Tau-381 protein. And the commercial ELISA kit was also used for Tau protein detection. It gave linearity range of 1.25×10^{-13} M~4.0×10^{-12} M with LOD 1.7×10^{-14} M. It shows that this ELA-PEC biosensor is sensitive.

Figure 4 Here

3.6 Selectivity and intermediate precision

Selectivity, stability and intermediate precision are significant methods to determine the performance of ELA-PEC biosensor. Simultaneously, several kinds of proteins, such as HSA, Tau-410, Tau-441, and AAT protein were used as nonspecific proteins to estimate the selectivity of the ELA-PEC biosensor. As shown in **Figure S8 (A)**. It can be seen from the diagram that this ELA-PEC biosensor has a good selectivity to Tau-381 protein. In addition, the intermediate precision of the ELA-PEC biosensor was also

evaluated. Due to the intermediate precision the PEC signal of the six parallel electrodes didn′t have obvious difference. As shown in **Figure S8 (B)**. Their photocurrent responses are 2086.6 nA, 2097.7 nA, 2100.2 nA, 2136.5 nA, 2027.4 nA, 2013.3 nA, respectively. And the corresponding relative standard deviation (RSD) was 2.27%. It showed the excellent intermediate precision of this ELA-PEC biosensor. As shown in **Figure S8 (C)**, the stability of this ELA-PEC biosensor was also determined. This ELA-PEC biosensor was stored for 0 day, 7 day, 14 day, 21 day and 28 day at 4 °C before the next detection. This storage period is up to 28 days. And the photocurrent response of the ELA-PEC biosensor decreases slowly. The photocurrent response measured after the storage of 28 days only has 7.2% reducing compared with the storage of 0 day. The result showed that this ELA-PEC biosensor has excellent stability. More data about intermediate accuracy is in **Table S1** of **Supporting Information**.

3.7 Real sample detection

In order to estimate the practical application performance of this ELA-PEC biosensor, the different concentrations of Tau-381 protein was added to the human serum which was diluted 100-fold with 0.1 M phosphate buffer. The diluted serum of healthy people and AD′s patient (one healthy people and three AD′s patients) were detected by using this ELA-PEC biosensor. And the result suggested the Tau-381 protein concentration of an AD patient is higher than the concentration of a healthy person (Sample 1) (**Table S2**). In the AD group (Sample 2, 3, 4), the average concentrations of tau-381 protein were 69.32 pM, 197.81 pM and 321.37 pM (n = 7), respectively. The recoveries were between 96.6% and 103.1%. According to the statistical analysis of the results it indicated no significant difference in the performance of the compared methods in accuracy or precision. The results indicated that this ELA-PEC biosensor can be used to accuracy detect the Tau-381 protein and has potential application value in complex blood samples. Statistical analysis of the results obtained by ELA-PEC biosensor, and those given by the comparison method was performed using the Student`s *t*-test and the variance ratio *F*-test. As illustrated in **Table S2**, the calculated values did not exceed the theoretical ones, indicating no significant difference in the performance of the compared methods in accuracy or precision.

3.8 Mechanism of the PEC response

As shown in **Scheme S1**, there is a feasible mechanism of this ELA-PEC biosensor. CB was conduction band and VB was valence band. There is a charge carrier transition between the $MoSe_2$NSs and the CPE. On the basis of the experimental results discussed above, it is believed that the increase of photocurrent response is closely related to the concentration of AA, which is confirmed by **Section 3.3.** AA is the electron donor, along with the $MoSe_2$NSs can produce an increased photocurrent response. The AuNPs/$MoSe_2$NSs/CPE without AA only generated a low photocurrent response about 189.7 nA. And when the AA was produced, the photocurrent response was increased to 2042.6 nA (5.0 pM target). The result shows that the photocurrent can be increased by contributing electrons to the valence band. It illustrated that AA is indispensable in the ELA-PEC biosensor. When the AuNPs/$MoSe_2$NSs/CPE was under irradiation, light

induced the electrons of $MoSe_2$NSs were excited from the occupied VB to the empty CB, meanwhile leaving electron holes in the VB. And at the same time electron-hole (e^-−h^+) pair was generated. In order to produce stable photocurrent response, AA as electron donor is essential. AA can inhibit the corrosion of $MoSe_2$NSs under irradiation. Electrons generated in CB of $MoSe_2$NSs are transferred to CPE to produce an anodic photocurrent and resulting in a large PEC response [29]. To prove this, PEC responses of photoelectrode in the presence of AAP with or without $MoSe_2$NSs was done. It suggested that the AuNPs/$MoSe_2$NSs/CPE has good PEC response in the presence of AAP (**Figure S10**).

Conclusions

In conclusion, this work successfully devised an enzyme linked aptamer photoelectrochemical biosensor for Tau-381 protein detection. It has a low detection limit of 0.3 fM and high selectivity compared with commercial ELISA kits. And it was the first time to detect Tau-381 protein using a PEC biosensor. In addition, although the strategy focused on the detection of Tau-381 protein, the ELA-PEC biosensor has good potential for detection of the other proteins. It is believed that this work provided a promising protocol for Tau-381 protein detection with high selectivity. And this strategy was also helpful for future ELA-PEC biosensor development.

Author statement

Xiaohui Kong: Conceptualization, Methodology, Writing- Reviewing, Formal analysis, Data curation, Writing-Original draft preparation, Visualization, Investigation. **Xu Hun:** Supervision, Validation, Writing- Reviewing and Editing, Project administration, Funding acquisition.

Conflict of Interest

The authors declared that they have no conflicts of interest to this work.

Acknowledgements

This work was supported by National Natural Science Foundation of China (21575073) and Laoshan Scholar Program of Qingdao University of Science and Technology (201802685).

References

[1] M. Heneka, An immune-cell signature marks the brain in Alzheimer`s disease, Nature 577(7790) (2020) 322-323.

[2] A. Grubman, G. Chew, J.F. Ouyang, G. Sun, X.Y. Choo, C. McLean, R.K. Simmons, S. Buckberry, D.B. Vargas-Landin, D. Poppe, J. Pflueger, R. Lister, O.J.L. Rackham, E. Petretto, J.M. Polo, A single-cell atlas of entorhinal cortex from individuals with Alzheimer's disease reveals cell-type-specific gene expression regulation, Nat. Neurosci. 22(12) (2019) 2087-2097.

[3] D. Gate, N. Saligrama, O. Leventhal, A.C. Yang, M.S. Unger, J. Middeldorp, K. Chen, B. Lehallier, D. Channappa, M.B. De Los Santos, A. McBride, J. Pluvinage, F. Elahi, G.K.-Y. Tam, Y. Kim, M. Greicius, A.D. Wagner, L. Aigner, D.R. Galasko, M.M. Davis, T. Wyss-Coray, Clonally expanded CD8 T cells patrol the cerebrospinal fluid in Alzheimer's disease, Nature 577(7790) (2020) 399-404.

[4] L. Yang, Y. Zhai, Y. Hao, Z. Zhu, G. Cheng, The Regulatory Functionality of Exosomes Derived from hUMSCs in 3D Culture for Alzheimer's Disease Therapy, Small 16(3) (2020) 1906273.

[5] X. Bai, S. Wang, X. Yan, H. Zhou, J. Zhan, S. Liu, V.K. Sharma, G. Jiang, H. Zhu, B. Yan, Regulation of Cell Uptake and Cytotoxicity by Nanoparticle Core under the Controlled Shape, Size, and Surface Chemistries, ACS Nano 14(1) (2020) 289-302.

[6] H. Ijaz, R. Zia, A. Taj, F. Jameel, F.K. Butt, T. Asim, N. Jameel, W. Abbas, M. Iqbal, S.Z. Bajwa, W.S. Khan, Synthesis of BiOCl nanoplatelets as the dual interfaces for the detection of glutathione linked disease biomarkers and biocompatibility assessment in vitro against HCT cell lines model, Applied Nanoscience 10(9) (2020) 3569-3576.

[7] M. Baghayeri, M. Nodehi, A. Amiri, N. Amirzadeh, R. Behazin, M.Z. Iqbal, Electrode designed with a nanocomposite film of CuO Honeycombs/Ag nanoparticles electrogenerated on a magnetic platform as an amperometric glucose sensor, Anal. Chim. Acta 1111 (2020) 49-59.

[8] S. Mei, B. Liu, X. Xiong, X. Hun, One-step fabrication of trimetallic alloy nanozyme catalyzer for luminol-H2O2 chemiluminescence and its application for miRNA-21 detection coupled with miRNA walking machine, J. Pharm. Biomed. Anal. 186 (2020) 113280.

[9] P. Manaswiyoungkul, F. Erdogan, O.O. Olaoye, A.D. Cabral, E.D. de Araujo, P.T. Gunning, Optimization of a high-throughput fluorescence polarization assay for STAT5B DNA binding domain-targeting inhibitors, J. Pharm. Biomed. Anal. 184 (2020) 113182.

[10] S. Yotsumoto Neto, M.I. Sousa Lima, S.R. Ferreira Pereira, L.R. Goulart, R. de

Cássia Silva Luz, F.S. Damos, Immunodiagnostic of leprosy exploiting a photoelectrochemical platform based on a recombinant peptide mimetic of a Mycobacterium leprae antigen, Biosens. Bioelectron. 143 (2019) 111625.

[11] X. Wang, X. Bai, Z. Pang, J. Zhu, Y. Wu, H. Yang, Y. Qi, X. Wen, Surface-enhanced Raman scattering by composite structure of gold nanocube-PMMA-gold film, Opt. Mater. Express 9(4) (2019) 1872-1881.

[12] S. Kim, A.W. Wark, H.J. Lee, Femtomolar Detection of Tau Proteins in Undiluted Plasma Using Surface Plasmon Resonance, Anal. Chem. 88(15) (2016) 7793-7799.

[13] Y. Gao, Y. Zhou, R. Chandrawati, Metal and Metal Oxide Nanoparticles to Enhance the Performance of Enzyme-Linked Immunosorbent Assay (ELISA), ACS Appl. Nano Mater. 3(1) (2020) 1-21.

[14] W. Jing, Y. Wang, Y. Yang, Y. Wang, G. Ma, S. Wang, N. Tao, Time-Resolved Digital Immunoassay for Rapid and Sensitive Quantitation of Procalcitonin with Plasmonic Imaging, ACS Nano 13(8) (2019) 8609-8617.

[15] V. Krivitsky, M. Zverzhinetsky, A. Krivitsky, L.-C. Hsiung, V. Naddaka, I. Gabriel, S. Lefler, J. Conroy, L. Burstein, F. Patolsky, Cellular Metabolomics by a Universal Redox-Reactive Nanosensors Array: From the Cell Level to Tumor-on-a-Chip Analysis, Nano Lett. 19(4) (2019) 2478-2488.

[16] F.D. Morris, E.M. Peterson, J.M. Heemstra, J.M. Harris, Single-Molecule Kinetic Investigation of Cocaine-Dependent Split-Aptamer Assembly, Anal. Chem. 90(21) (2018) 12964-12970.

[17] J. Ge, L. Fan, J. Wang, Q. Zhang, Z. Liu, E. Zhang, Q. Liu, X. Yu, B. Lu, MoSe2/N-Doped Carbon as Anodes for Potassium-Ion Batteries, Advanced Energy Materials 8(29) (2018) 1801477.

[18] E.M. Alexeev, D.A. Ruiz-Tijerina, M. Danovich, M.J. Hamer, D.J. Terry, P.K. Nayak, S. Ahn, S. Pak, J. Lee, J.I. Sohn, M.R. Molas, M. Koperski, K. Watanabe, T. Taniguchi, K.S. Novoselov, R.V. Gorbachev, H.S. Shin, V.I. Fal'ko, A.I. Tartakovskii, Resonantly hybridized excitons in moiré superlattices in van der Waals heterostructures, Nature 567(7746) (2019) 81-86.

[19] M. Sakthivel, R. Sukanya, S.-M. Chen, B. Dinesh, Synthesis of Two-Dimensional Sr-Doped MoSe2 Nanosheets and Their Application for Efficient Electrochemical Reduction of Metronidazole, The Journal of Physical Chemistry C 122(23) (2018) 12474-12484.

[20] Y. Zhang, H. Zhu, L. Yu, J. He, C. Huang, MoSe2 modified TiO2 nanotube arrays with superior photoelectrochemical performance, Mater. Res. Express 5(4) (2018) 045014.

[21] Y. Li, X. Li, Y. Meng, X. Hun, Photoelectrochemical platform for MicroRNA let-7a detection based on graphdiyne loaded with AuNPs modified electrode coupled with alkaline phosphatase, Biosens. Bioelectron. 130 (2019) 269-275.

[22] Y. Liu, M. Pan, W. Wang, Q. Jiang, F. Wang, D.-W. Pang, X. Liu, Plasmonic and Photothermal Immunoassay via Enzyme-Triggered Crystal Growth on Gold Nanostars, Anal. Chem. 91(3) (2019) 2086-2092.

[23] T. Yao, X. Hun, A design for the photoelectrochemical detection of miRNA-221 based on a tungsten diselenide–cysteine–dopamine nanoprobe coupled with mismatched catalytic hairpin assembly target recycling with ultra-low background noise, Chem. Commun. 55(70) (2019) 10380-10383.

[24] B. Shui, D. Tao, J. Cheng, Y. Mei, N. Jaffrezic-Renault, Z. Guo, A novel electrochemical aptamer–antibody sandwich assay for the detection of tau-381 in human serum, Analyst 143(15) (2018) 3549-3554.

[25] S.X. Wang, D. Acha, A.J. Shah, F. Hills, I. Roitt, A. Demosthenous, R.H. Bayford, Detection of the tau protein in human serum by a sensitive four-electrode electrochemical biosensor, Biosens. Bioelectron. 92 (2017) 482-488.

[26] A. Zengin, U. Tamer, T. Caykara, A SERS-Based Sandwich Assay for Ultrasensitive and Selective Detection of Alzheimer's Tau Protein, Biomacromolecules 14(9) (2013) 3001-3009.

[27] X. Zhang, S. Liu, X. Song, H. Wang, J. Wang, Y. Wang, J. Huang, J. Yu, Robust and Universal SERS Sensing Platform for Multiplexed Detection of Alzheimer's Disease Core Biomarkers Using PAapt-AuNPs Conjugates, ACS Sensors 4(8) (2019) 2140-2149.

[28] L. Chen, J. Lin, J. Yi, Q. Weng, Y. Zhou, Z. Han, C. Li, J. Chen, Q. Zhang, A tyrosinase-induced fluorescence immunoassay for detection of tau protein using dopamine-functionalized CuInS2/ZnS quantum dots, Anal. Bioanal. Chem. 411(20) (2019) 5277-5285.

[29] X. Hun, X. Xiong, J. Ding, W. Qin, Photoelectric current as a highly sensitive readout for potentiometric sensors, Chem. Commun. 56(27) (2020) 3879-3882.

Figure Captions

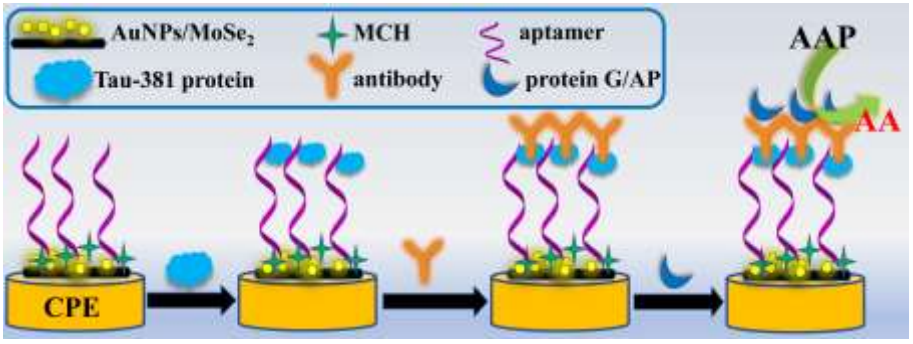

Scheme 1. Schematic illustration of enzyme linked aptamer PEC biosensor for Tau-381 protein.

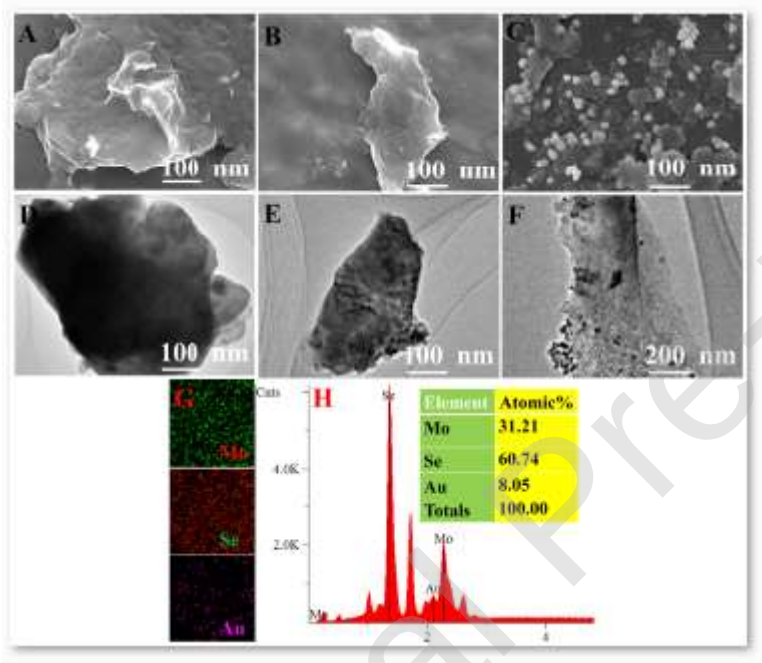

Figure 1 SEM images of bulk $MoSe_2$ (A), $MoSe_2$NSs (B) and AuNPs/$MoSe_2$NSs (C); TEM images of bulk $MoSe_2$ (D), $MoSe_2$NSs (E) and AuNPs/$MoSe_2$NSs (F). Elemental mapping image of AuNPs/$MoSe_2$NSs (G). EDS of AuNPs/$MoSe_2$NSs (H).

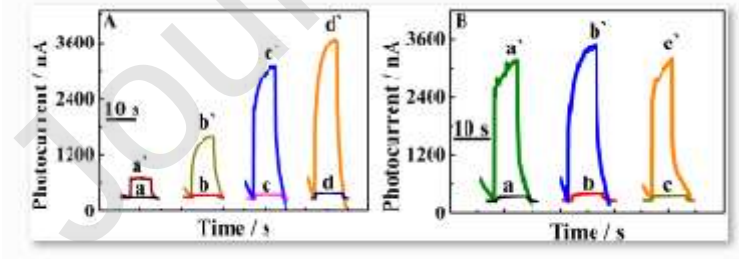

Figure 2. PEC response of bare CPE (a, a`), bulk $MoSe_2$/CPE (b, b`), $MoSe_2$NSs/CPE (c, c`), AuNPs/$MoSe_2$NS/CPE (d, d`) (A). The effect of the mass ratio of $MoSe_2$NSs to chloroauric acid on PEC response, 1:3.75 (a, a`), 1:2.5 (b, b`), 1:1.875 (c, c`) (B). a, b, c, d: PEC performance in Tris-HCl (pH 7.4) without AA; a`, b`, c`, d`: PEC performance in Tris-HCl (pH 7.4) contained 0.1 M AA.

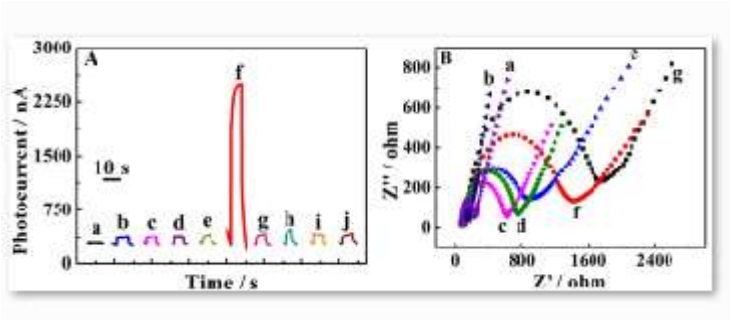

Figure 3 (A) PEC responses of different electrode incubated with 0.1 M AAP. a: bare CPE; b: AuNPs/$MoSe_2$NSs/CPE; c: aptamer/AuNPs/$MoSe_2$NSs/CPE; d: Tau-381 protein/MCH/aptamer/AuNPs/$MoSe_2$NSs/CPE; e: antibody/Tau-381 protein/MCH/aptamer/AuNPs/$MoSe_2$NSs/CPE; f: protein G/AP/antibody Tau-381 protein/MCH/aptamer/AuNPs/$MoSe_2$NSs/CPE (5.0 pM target), g: (0 fM target), h (0.3 fM target), i: (0.1 fM) (g, h and i: the condition is same with f except the concentration is different); j: protein G/AP/antibody Tau-381 protein/MCH/aptamer/ AuNPs/$MoSe_2$NSs/CPE without AAP (5.0 pM target). **(B)** Nyquist plot of different electrode in 0.1 M KCl solution contained 5.0 mM $[Fe(CN)_6]^{3-/4-}$. a: bare CPE; b: AuNPs/$MoSe_2$NSs/CPE; c: aptamer/AuNPs/$MoSe_2$NSs/CPE; d: MCH/aptamer/AuNPs/$MoSe_2$NSs/CPE; e: Tau-381 protein/MCH/aptamer/AuNPs/$MoSe_2$NSs/CPE; f: antibody/Tau-381 protein MCH/aptamer/AuNPs/$MoSe_2$NSs/CPE; g: protein G/AP/antibody Tau-381 protein MCH/aptamer/AuNPs/$MoSe_2$NSs/CPE. The mass ratio of $MoSe_2$NSs and chloroauric acid is 1:2.5

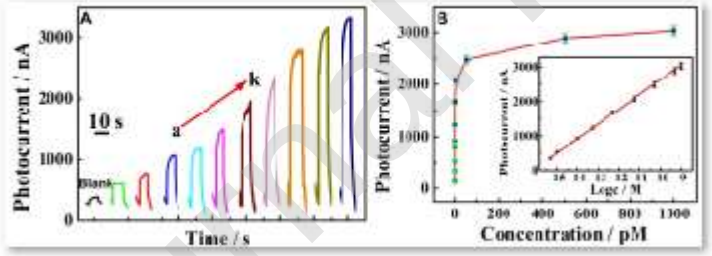

Figure 4 PEC responses of the ELA-PEC biosensor toward different concentrations of Tau-381 protein. From a to k: 0 fM, 0.5 fM, 1.0 fM, 5.0 fM, 10.0 fM, 50.0 fM, 500.0 fM, 5.0 pM, 50.0 pM, 500.0 pM, 1.0 nM **(A)**. The PEC responses to the concentration of Tau-381 protein **(B)**. The linear relationship of the PEC responses to the logarithm of Tau-381 protein concentration (Insert).

Table Captions

Table 1 Performance comparison of this ELA-PEC biosensor with other methods for Tau protein detection.

Target	Signal source [a]	Method	Linearity range	LOD	Ref
Tau-381	Aptamer-Tau	SPR	2 pM - 80 pM	10 fM	[12]
Tau-381	AuNPs-CS [b]	EC	0.5 pM - 0.1 nM	0.42 pM	[24]
Tau	Ab-Ag	EC	~ - 500 n M	30 fM	[25]
Tau	Ab-AuNPs	SERS	25 fM - 500 n M	25 fM	[26]
Tau-381	PAapt-AuNPs	SERS	1 fM - 3 n M	0.42 fM	[27]
Tau-381	$CuInS_2$/ZnS-DA [d]	Flu	10 pM - 200 nM	9.3 pM	[28]
Tau-381	AuNPs/$MoSe_2$-AA	PEC	0.5 fM - 1.0 nM	0.3 fM	[c]

[a] The generation method of the detection signal. [b] CS, cysteamine; Ab, antibody; Ag, antigen; PAapt-AuNPs, Dye-coded polyA (polyadenine) aptamer-AuNPs conjugates; $CuInS_2$/ZnS-DA, Dopamine-functionalized $CuInS_2$/ZnS QDs. EC; Electrochemical; SPR, Surface plasmon resonance; SERS, Surface enhanced Raman scattering; Flu, Fluorescence; PEC, Photoelectrochemical. [c] This work